ASTRONOMY & ASTROPHYSICS
SUPPLEMENT SERIES

Astron. Astrophys. Suppl. Ser. **129,** 399-412 (1998)

The ESO Nearby Abell Cluster Survey⋆,⋆⋆,⋆⋆⋆

V. The catalogue: Contents and instructions for use

P. Katgert[1], **A. Mazure**[2], **R. den Hartog**[1,3], **C. Adami**[2], **A. Biviano**[1,4], **and J. Perea**[5]

[1] Sterrewacht Leiden, The Netherlands
[2] IGRAP, Laboratoire d'Astronomie Spatiale, Marseille, France
[3] ESTEC, SA Division, Noordwijk, The Netherlands
[4] ISO Science Team, ESA, Villafranca, Spain
[5] Instituto de Astrofísica de Andalucía, CSIC, Granada, Spain

Received June 16; accepted October 14, 1997

Abstract. We present the catalogue resulting from the ESO Nearby Abell Cluster Survey (the ENACS), which contains redshifts and magnitudes for 5634 galaxies in the directions of 107 rich, nearby southern Abell cluster candidates. We describe the contents of the catalogue and discuss the results of a comparison between the ENACS catalogue and the COSMOS Galaxy Catalogue.

When cross-correlating the two catalogues we find that, at least in the areas of the ENACS clusters, the completeness of the COSMOS catalogue is somewhat lower than was estimated previously for the carefully analyzed and well-calibrated part of the COSMOS catalogue known as the Edinburgh-Durham Southern Galaxy Survey (EDSGC).

The galaxy positions in the COSMOS and ENACS catalogues are found to be on the same system to within about one arcsecond.

For the clusters for which the photometry in the ENACS and COSMOS catalogues is based on the same survey plates, the two magnitude scales agree very well. We confirm that the photometric calibration in the EDSGC subset of the COSMOS catalogue is of higher quality than in the EDSGC complement.

The ENACS galaxy samples are unbiased subsets of the COSMOS catalogue as far as the projected galaxy distribution is concerned, except in only a few cases. We summarize how the ENACS galaxy samples are subsets of the COSMOS catalogues in the ENACS apertures, with respect to magnitude. For the ENACS catalogue as a whole, we describe the apparent incompleteness at faint magnitudes and towards higher redshifts. Finally, we provide some detailed information about the ENACS catalogue that is essential for its proper statistical use and we summarize some facts that must be remembered when selecting subsets of galaxies from it.

Key words: galaxies: clusters — galaxies: redshifts — galaxies: photometry — catalogs

1. Introduction

Ever since the pioneering work of Abell (1958), it has been realized that the study of clusters of galaxies holds great promise of providing clues to several fundamental problems in Cosmology. The global properties and the internal structure of clusters contain information about their formation and evolution and therefore, indirectly, about several of the parameters of the scenario for the formation of large-scale structure. At this moment cluster properties are determined from essentially four types of observation: the projected galaxy distribution, the kinematics of the cluster galaxies, the distribution of the density and temperature of the hot X-ray emitting gas and, finally, the surface density of the total gravitating mass (galaxies, gas and dark matter) as derived from gravitational lensing.

In the late seventies the first systematic cluster redshift surveys were made for the nearest and most conspicuous clusters, such as Coma (e.g. Kent & Gunn 1982). In the early eighties, the first extensive cluster redshift surveys were done of *samples* of rich clusters, for each of which, on average, of order 100 redshifts were obtained (e.g. Dressler & Shectman 1988). These redshift surveys

Send offprint requests to: P. Katgert

⋆ Based on observations collected at the European Southern Observatory (La Silla, Chile).

⋆⋆ http://www.astrsp-mrs.fr/www/enacs.html

⋆⋆⋆ Tables 2 and 5, as well as the full ENACS catalogue are only available in electronic form at the CDS via anonymous ftp to cdsarc.u-strasbg.fr (130.79.128.5) or via http://cdsweb.u-strasbg.fr/Abstract.html

used galaxy catalogues of cluster member candidates especially prepared for these clusters (e.g. the photometric catalogue by Godwin & Peach 1977, for the Coma cluster, or the catalogues by Dressler 1980, used by Dressler & Shectman).

Most of the early redshift work on clusters employed slit-spectroscopy of individual galaxies. However, several kinds of multi-object spectrographs have become available in the last ten years or so. This has accelerated cluster redshift surveys by factors between, say 10 and 100. As a result, extensive redshift surveys for large *samples* of clusters have become possible. This allows a detailed study of the dynamics of galaxy clusters as a *species*, from a combination of kinematical data with surface density profiles, X-ray data and evidence from lensing. By themselves, the redshift surveys also enable one to study possible kinematical differences between different types of cluster galaxies, and structure in the phase space of clusters, both of which may give important clues about the formation and dynamical evolution of clusters.

At ESO, the Optopus multi-object fibre spectrograph was developed in the mid eighties (see e.g. Lund 1986 or Avila et al. 1989). It employs aperture plug plates at the Cassegrain focus of the 3.6-m telescope. With its aperture plate size of $\approx 30'$ it was ideally suited to redshift surveys of the central regions of rich and not-too-nearby clusters. In this paper, we present the redshift catalogue that has resulted from a survey with the Optopus spectrograph of about 100 rich southern clusters in the redshift range from $\sim$0.04 to $\sim$0.1. The spectroscopic observations took place during about 35 nights in 9 observing runs in the period September 1989 to October 1993.

We have already discussed several aspects of the observations and the data analysis of the survey which has resulted in the catalogue that we present here (see Katgert et al. 1996, Paper I), and which we will refer to as the ENACS catalogue. We have also discussed several results based on the ENACS catalogue, e.g. the distribution of the velocity dispersions of a volume-limited complete sample of rich Abell clusters (Mazure et al. 1996, Paper II), and the kinematics of emission-line galaxies (Biviano et al. 1997, Paper III). In addition, the ENACS data have also been used to study the kinematics and dynamics of the galaxies in the cores of rich clusters (den Hartog & Katgert 1996; den Hartog 1997).

A few other papers have been submitted, e.g. on the Fundamental Plane of clusters (Adami et al. 1997), on the density profiles of clusters (Adami et al. 1998) and on the distribution and kinematics of early- and late-type galaxies (de Theije & Katgert 1998). We are also working on several other aspects of the structure and dynamics of rich clusters, using the ENACS as a starting point. In addition, other groups have already used some of the ENACS data e.g. to make an independent study of the distribution of cluster velocity dispersions (Fadda et al. 1996), to study substructure in the distribution of the cluster galaxies (Girardi et al. 1997), and to construct the power spectrum on large scales (Borgani et al. 1997). Here, we present the total ENACS catalogue to enable other workers in the field to take full advantage of all aspects of our dataset.

2. The catalogue

The main objective of the ENACS programme was to drastically increase the number of redshifts for galaxies in rich Abell clusters. The direct goal was to construct a complete, volume-limited sample of at least 100 rich Abell clusters, for which the ENACS data, in combination with data already in the literature, would provide good kinematical data. Consequently, the main observational effort of the ENACS consisted of multi-object spectroscopy. In addition, CCD-imaging was done to calibrate the photographic photometry which formed the basis for the selection of the galaxies to be observed spectroscopically.

In Paper I we have discussed the definition of the cluster sample, and the selection of the galaxies in the direction of the clusters to be observed with Optopus. In that paper, we also described the methods employed in the determination of the redshifts, and of the magnitudes. Here we present the positions and redshifts of all 5634 ENACS galaxies, as well as the red magnitudes of 5615 ENACS galaxies, and we give the estimated errors in the redshift estimates. For the redshifts derived from absorption lines using cross-correlation with template spectra (see Paper I, and Tonry & Davis 1979), we also give the S/N-ratio of the peak in the correlation function. As shown in Paper I, this S/N-ratio allows one to estimate the reliability of the redshift. For about one-fifth of the galaxies we could estimate the redshift from emission lines, either exclusively or in addition to an absorption-line redshift. For all galaxies with clear emission lines in the spectrum, we give information about which lines were seen, and the approximate line ratios (using an excitation code) as well as on the presence or absence of features in the continuum.

In Table 1 we show a summary of the catalogue; the total catalogue is available electronically from the CDS (and by anonymous ftp from: 132.229.214.2 as pub/katgert/enacs.cat, or from: 193.50.128.3 as amazure/enacs/enacs.cat). In Table 1 we give the results for *one galaxy in each of the redshift surveys* in the direction of the 107 target ACO clusters. By choosing the last entry in each survey we implicitly show the total number of redshifts measured towards a cluster.

The organization of Table 1 is as follows:
Column (1): sequence number of cluster in ACO catalogue (Abell et al. 1989)
Column (2): sequence number of galaxy in redshift survey of cluster (= total number of redshifts in the survey)
Column (3): right ascension (equinox 1950.0)
Column (4): declination (equinox 1950.0)

Table 1. Summary of the ENACS catalogue

Abell	nr.	$\alpha(1950)$	$\delta(1950)$	R_{25}	cz	δ_{cz}	$cz_{\rm abs}$	S/N	$cz_{\rm emi}$	LC	EC	CI
0013	44	00:12:17.38	−19:57:53.3	16.41	39595	96	39595	2.39	0	0	0	0
0087	42	00:40:59.51	−10:08:12.0	17.07	16746	40	0	0.00	16746	6	3	2
0118	38	00:53:47.33	−26:42:03.6	16.47	12367	51	12377	2.23	12357	6	3	3
0119	118	00:55:06.39	−01:09:44.7	16.48	12478	48	12478	4.99	0	0	0	0
0151	112	01:08:13.33	−15:47:09.0	14.44	9214	51	9214	5.25	0	0	0	0
0168	100	01:13:54.35	−00:17:50.3	16.62	32024	102	32024	2.04	0	0	0	0
0229	39	01:37:33.26	−03:47:59.3	16.96	33322	75	33322	3.18	0	0	0	0
0295	43	02:00:44.56	−01:14:27.6	15.88	38505	75	38505	3.53	0	0	0	0
0303	16	02:04:25.03	−03:24:09.1	16.76	36618	93	36618	2.39	0	0	0	0
0367	30	02:35:11.57	−19:28:52.2	16.02	28018	102	28018	2.00	0	0	0	0
0380	41	02:43:15.10	−26:28:36.7	17.23	41145	117	41145	1.77	0	0	0	0
0420	33	03:07:58.18	−11:41:22.3	17.09	25860	47	25863	2.68	25857	5	0	3
0514	111	04:47:41.41	−20:53:40.0	17.52	32679	40	0	0.00	32679	7	2	3
0524	43	04:56:45.68	−19:48:11.4	17.30	21955	43	21875	3.16	22035	5	0	2
0543	24	05:29:29.12	−22:19:04.9	17.97	25487	75	25487	3.38	0	0	0	0
0548	297	05:48:33.69	−25:28:39.5	15.15	25087	72	25087	3.27	0	0	0	0
0754	39	09:07:19.12	−09:26:21.9	16.05	15540	75	15540	2.89	0	0	0	0
0957	36	10:12:06.39	−00:34:53.6	13.28	14914	81	14914	2.55	0	0	0	0
0978	73	10:18:58.09	−06:28:28.2	15.28	16370	51	16370	4.56	0	0	0	0
1069	40	10:37:59.88	−08:15:10.1	16.33	20086	66	20086	3.53	0	0	0	0
1809	32	13:51:08.22	05:30:58.0	15.35	24092	66	24092	3.48	0	0	0	0
2040	43	15:11:05.05	07:24:46.1	15.39	12293	47	12339	4.85	12247	4	0	3
2048	39	15:13:24.43	04:37:52.7	16.44	29460	78	29460	2.90	0	0	0	0
2052	39	15:15:09.08	07:13:16.0	15.40	10069	48	10069	4.77	0	0	0	0
2353	31	21:32:45.14	−01:53:17.8	17.41	20214	43	20216	3.34	20212	7	2	0
2354	14	21:34:05.41	−15:04:06.8	17.87	26658	81	26658	3.04	0	0	0	0
2361	33	21:37:17.65	−14:37:17.9	17.48	18365	60	18365	4.12	0	0	0	0
2362	27	21:39:16.44	−14:17:57.0	16.23	14764	78	14764	2.80	0	0	0	0
2383	25	21:50:31.07	−21:22:15.8	16.94	39457	87	39457	2.62	0	0	0	0
2401	30	21:56:22.94	−20:29:33.6	16.80	27572	66	27572	3.65	0	0	0	0
2426	36	22:12:36.77	−10:30:17.6	16.67	29862	66	29862	4.02	0	0	0	0
2436	19	22:19:01.40	−03:10:35.8	16.11	17178	51	17178	4.73	0	0	0	0
2480	18	22:44:07.60	−17:57:23.0	16.50	8670	40	0	0.00	8670	6	4	1
2500	36	22:51:46.38	−25:40:06.2	17.30	27087	66	27087	3.82	0	0	0	0
2502	2	22:53:39.33	−16:50:37.8	13.44	2919	40	0	0.00	2919	6	3	3
2569	41	23:16:13.85	−13:01:29.2	16.72	24348	57	24348	4.35	0	0	0	0
2644	35	23:38:43.70	−00:14:25.6	17.70	55833	80	0	0.00	55833	1	0	0
2715	34	23:59:57.72	−34:41:44.0	17.25	33635	84	33635	2.69	0	0	0	0
2717	53	23:59:59.36	−36:33:15.1	14.26	14498	66	14498	3.81	0	0	0	0
2734	116	00:10:53.59	−29:11:50.2	17.46	19013	72	19013	3.18	0	0	0	0
2755	36	00:16:25.52	−35:25:53.9	16.96	34971	81	34971	2.77	0	0	0	0
2764	24	00:19:16.81	−49:28:08.0	16.61	48284	105	48284	2.47	0	0	0	0
2765	28	00:19:49.67	−20:52:51.4	15.91	26586	87	26586	2.76	17122	2	0	0
2778	40	00:27:08.64	−30:31:38.0	15.63	23530	57	23530	4.46	0	0	0	0
2799	42	00:36:10.63	−39:24:45.1	15.73	18886	105	18886	1.87	0	0	0	0
2800	46	00:36:52.74	−25:13:28.7	16.66	31247	75	31247	3.20	0	0	0	0
2819	124	00:46:35.18	−63:43:10.6	16.71	32521	56	32643	1.99	32399	3	1	1
2854	35	00:59:43.12	−50:55:27.2	15.23	18087	54	18087	4.41	0	0	0	0
2871	40	01:06:43.02	−37:06:32.7	17.14	38621	87	38621	2.86	0	0	0	0
2911	44	01:25:01.92	−38:18:52.8	17.15	24630	66	24630	3.88	0	0	0	0
2915	7	01:26:40.10	−29:17:52.1	15.02	26092	75	26092	3.04	0	0	0	0
2923	33	01:31:07.88	−31:30:09.4	16.33	38937	78	38937	2.94	0	0	0	0
2933	11	01:40:33.39	−54:50:08.0	16.16	28058	117	28058	1.69	0	0	0	0
2954	24	01:55:01.39	−71:29:46.5	17.66	66373	80	0	0.00	66373	1	1	1
3009	16	02:21:30.65	−48:44:09.4	15.85	22301	51	22301	5.55	0	0	0	0
3093	40	03:10:31.67	−47:34:35.4	16.79	24805	54	24805	4.90	0	0	0	0
3094	99	03:12:08.41	−27:06:06.1	18.08	31926	40	0	0.00	31926	3	1	2
3108	14	03:14:06.52	−47:54:40.5	15.91	18606	51	18606	5.27	0	0	0	0
3111	48	03:17:27.76	−45:54:26.0	16.82	43683	102	43683	2.38	0	0	0	0
3112	102	03:18:25.68	−44:17:02.3	16.93	39569	108	39569	1.91	0	0	0	0
3122	119	03:21:39.91	−41:33:09.2	15.68	20067	54	20067	4.55	0	0	0	0
3128	193	03:32:00.91	−52:40:26.5	16.20	17649	63	17649	3.72	0	0	0	0
3141	22	03:35:10.44	−28:10:21.2	16.32	31400	66	31400	4.08	0	0	0	0
3142	38	03:36:11.47	−39:59:06.5	16.62	31842	81	31842	3.14	0	0	0	0
3144	3	03:34:42.83	−55:21:50.9	16.47	13250	93	13250	2.18	0	0	0	0
3151	43	03:39:06.74	−29:00:13.1	17.04	26921	40	0	0.00	26921	7	3	3
3158	122	03:44:23.33	−53:47:12.0	16.34	30435	117	30435	1.95	0	0	0	0
3194	33	03:57:47.39	−30:12:32.1	15.29	30382	62	30267	1.68	30497	5	0	2
3202	41	04:00:29.85	−53:43:09.9	13.89	11505	55	11504	2.98	11506	2	0	3
3223	110	04:08:34.14	−31:00:41.2	14.61	21118	48	21152	4.95	21084	1	0	0
3264	11	04:31:15.08	−49:22:37.0	16.42	31797	40	0	0.00	31797	3	0	0
3301	7	04:59:50.35	−38:48:26.6	13.78	16093	72	16093	3.16	0	0	0	0
3341	118	05:25:20.64	−31:54:35.1	16.29	34302	78	34302	3.31	0	0	0	0
3354	110	05:34:50.36	−28:21:44.6	15.50	11033	40	0	0.00	11033	6	5	2
3365	35	05:47:06.84	−21:48:57.3	16.84	27101	69	27101	3.39	0	0	0	0

Table 1. continued

Abell	nr.	α(1950)	δ(1950)	R_{25}	cz	δ_{cz}	$cz_{\rm abs}$	S/N	$cz_{\rm emi}$	LC	EC	CI
3528	39	12:52:46.15	−28:52:22.7	15.09	21521	117	21521	1.52	0	0	0	0
3558	83	13:27:51.43	−31:24:51.6	14.40	13457	54	13457	4.37	0	0	0	0
3559	69	13:28:31.21	−29:05:31.0	14.14	14138	48	14138	5.02	0	0	0	0
3562	119	13:32:22.85	−31:18:25.5	14.52	13673	54	13673	4.18	0	0	0	0
3651	92	19:52:48.48	−55:19:59.5	15.82	18191	63	18191	4.12	0	0	0	0
3667	113	20:12:09.39	−57:21:52.9	16.68	16618	51	16618	5.12	0	0	0	0
3677	18	20:24:46.90	−33:32:00.5	16.42	31658	99	31658	2.44	0	0	0	0
3682	11	20:27:02.36	−37:05:55.4	16.63	27808	120	27808	1.75	0	0	0	0
3691	36	20:32:04.45	−38:14:05.3	16.63	5566	90	5566	2.16	14237	2	0	0
3693	33	20:31:59.55	−34:42:26.4	16.48	28067	66	28067	3.60	0	0	0	0
3695	96	20:33:09.37	−36:18:27.9	17.33	25863	44	25899	2.80	25827	7	3	3
3696	12	20:32:54.42	−35:12:52.5	16.31	26456	84	26456	3.04	0	0	0	0
3703	32	20:38:04.92	−61:30:26.4	15.31	21104	60	21104	4.34	0	0	0	0
3705	41	20:40:15.47	−35:26:02.3	16.56	33855	75	33855	3.21	0	0	0	0
3733	44	21:00:04.25	−28:19:06.5	16.21	11163	51	11163	4.93	0	0	0	0
3744	86	21:06:11.38	−25:45:35.7	14.50	8923	40	8917	3.15	8929	6	2	3
3764	43	21:23:52.32	−35:02:18.2	16.07	22123	47	22112	2.79	22134	3	1	2
3781	15	21:32:37.62	−66:56:11.8	17.70	21377	80	0	0.00	21377	1	0	0
3795	14	21:36:22.71	−32:24:40.7	16.00	27349	60	27349	4.71	0	0	0	0
3799	15	21:39:02.43	−72:49:36.7	14.23	14212	66	14212	3.39	0	0	0	0
3806	119	21:46:41.42	−57:38:45.9	16.84	41291	87	41291	2.69	0	0	0	0
3809	127	21:47:02.73	−44:01:13.6	15.88	15377	51	15377	4.62	0	0	0	0
3822	101	21:53:58.39	−57:47:59.8	16.25	22476	49	22472	2.66	22480	7	5	1
3825	90	21:56:43.41	−60:27:42.8	16.32	23090	63	23090	3.71	0	0	0	0
3827	22	21:59:07.15	−60:13:25.8	0.00	29730	87	29730	2.88	0	0	0	0
3864	41	22:18:19.18	−52:49:07.4	16.03	29872	45	29864	3.04	29880	3	0	0
3879	82	22:28:58.27	−69:28:29.1	16.33	20393	51	20393	5.09	0	0	0	0
3897	13	22:37:27.54	−17:40:15.2	16.62	22331	63	22331	4.30	0	0	0	0
3921	38	22:48:20.06	−64:38:35.1	16.35	27684	75	27684	3.11	0	0	0	0
4008	43	23:28:41.59	−39:37:43.7	16.99	48339	105	48339	2.03	0	0	0	0
4010	36	23:29:35.77	−36:48:06.0	16.19	29042	66	29042	3.68	0	0	0	0
4053	31	23:53:05.19	−27:58:28.0	15.95	15190	80	0	0.00	15190	2	0	0

Column (5): R_{25}, i.e. the isophotal R-magnitude within the 25 mag/arcsec^2 isophote (a value of 0.00 means: not available)

Column (6): the adopted heliocentric velocity, cz, of the galaxy

Column (7): the estimated error in the adopted heliocentric velocity

Column (8): the heliocentric velocity, $cz_{\rm abs}$, of the galaxy based on absorption lines (a value of 0 means: not available)

Column (9): the signal-to-noise ratio of the peak in the cross-correlation function used to derive $z_{\rm abs}$ (a value of 0.00 means: not available)

Column (10): the heliocentric velocity, $cz_{\rm emi}$, of the galaxy based on emission lines (a value of 0 means: not available)

Column (11): code indicating the presence of emission lines, LC, 0: no emission lines seen; 1: OII λ 3727; 2: Hβ; 3: OII λ 3727 + Hβ; 4: OIII λ 4959/5007; 5: OII λ 3727 + OIII λ 4959/5007; 6: Hβ + OIII λ 4959/5007; 7: OII λ 3727 + Hβ + OIII λ 4959/5007

Column (12): excitation code, EC, 0: not available; 1: Hβ > OIII λ 5007; 2: OIII λ 5007 > Hβ > OIII λ 4959; 3: Hβ ≈ OIII λ 4959; 4: Hβ < OIII λ 4959; 5: AGN (i.e.: very broad Hβ)

Column (13): continuum index, CI, (not given for spectra without emission lines) 0: not available; 1: featureless; 2: metallic absorption lines; 3: strong absorption under Hβ.

For a description of the methods employed in determining positions, magnitudes, redshifts and redshift errors we refer the reader to the relevant sections of Paper I. Note that among the 666 galaxies with both an emission- and an absorption-line redshift we have 80 cases in which the two redshift estimates are discordant (i.e. differ by more than 500 km/s). In these 80 cases we have derived the ENACS redshift according to a simple scheme which takes into account the estimated reliabilities for different categories of redshift estimates (see Sect. 4.3 in Paper I for more details). This scheme generally (but not always) selects the most probable value, but it does not take into account the redshifts of other galaxies in the cluster. Therefore, we list both redshift estimates.

While measuring the wavelengths of the emission lines, the relative intensities were also estimated. An indication of the line ratios is summarized in the Excitation Code. In view of the difficulties associated with estimating equivalent widths, especially for the narrow oxygen lines, the code in Col. 12 of Table 1 should be used with caution. On the other hand, the Excitation Code for AGN is thought to be quite reliable; in other words: this code was assigned only if there was little or no doubt about the AGN character of the ENACS spectrum of the object. As a consequence, it is possible that not every AGN in the catalogue has been assigned the AGN Excitation Code, because it

is not certain that we have been able to recognize unambiguously all AGN as such from their ENACS spectrum.

Finally, for the galaxies with emission lines in their spectrum, an indication is frequently (but not always) given about the presence or absence of features in the continuum spectrum. When this Continuum Index is 0, this simply means that the quality of the spectrum was not sufficient for a reliable statement about the character of the continuum.

After the spectroscopic observations for the ENACS were done, we became aware of published redshifts for 33 galaxies without ENACS redshift, in the "Optopus areas" of the four ENACS clusters A168, A957, A1809 and A2052. Most of these 33 galaxies (viz. 21 of them) were in the galaxy catalogues that we prepared for the Optopus observations, so that we have positions and magnitudes for them in the same systems as for the ENACS galaxies. Some of these galaxies had been observed by us with Optopus, but without yielding a redshift; others were not observed. The remaining 12 (predominantly faint) galaxies for which non-ENACS redshifts have been published were not in our galaxy catalogues, and no magnitudes are available for them.

As these galaxies may be of interest in certain types of analysis (some are among the brightest galaxies in their parent cluster), we have listed all 33 in Table 2. The organization of Table 2 is as follows:
Column (1): sequence number of cluster in the ACO catalogue (Abell et al. 1989)
Column (2): right ascension (equinox 1950.0)
Column (3): declination (equinox 1950.0)
Column (4): R_{25}, i.e. the isophotal R-magnitude within the 25 mag/arcsec^2 isophote (0.00 means: not available, i.e. the galaxy is not in the catalogue we prepared for the Optopus observations)
Column (5): the heliocentric velocity, cz, of the galaxy
Column (6): the estimated error in the heliocentric velocity
Column (7): reference to source of redshift.

3. Comparison with the COSMOS catalogue

At the start of the ENACS programme, the large-scale galaxy catalogues that are presently available in several flavours, like the COSMOS (e.g. Wallin et al. 1994) and the APM surveys (Maddox et al. 1990), and that are based on automatic scanning of photographic survey plates and subsequent computer processing, were not yet available. Therefore, we had to produce our own galaxy catalogues in the direction of the target ACO clusters, in preparation for the Optopus multi-object spectroscopy. The most important requirements that these cluster galaxy catalogues had to meet were that they should have very good positional quality (better than 1 arcsec), and that good photometry was available so that galaxy samples complete in apparent magnitude could be selected.

We prepared our cluster galaxy catalogues with the Leiden Observatory Astroscan automatic plate measuring machine. The positional quality, required for very good relative positioning of the Optopus fibres as well as to secure excellent positional consistency between galaxy and guide star fibres, could easily be met. The photometric requirement could not be met in an absolute sense, but the relative photometry of the Astroscan was known to be quite good. This allowed the definition of galaxy samples complete to a well-defined magnitude limit, the absolute value of which still had to be calibrated by photometric CCD imaging of well-chosen galaxy subsamples.

At the completion of the observational part of the ENACS programme, we have compared the ENACS positional and photometric systems with those of the COSMOS catalogue. Note that the latter contains a high-quality subset, the Edinburgh-Durham Southern Galaxy Catalogue, or EDSGC (Heydon-Dumbleton et al. (1989), for which the calibration is of higher quality than for the rest of the COSMOS catalogue, while its completeness has been studied in detail.

The comparison between the ENACS and COSMOS catalogues was made for only 77 of the 107 ENACS clusters, but this should not affect the general validity of the results. The 77 clusters in question are listed in Table 3. We have marked with an asterisk the 15 clusters within the EDSGC.

Table 3. ENACS clusters with COSMOS data

A0013	A0524	A2502	A2911*	A3144	A3733
A0087	A0543	A2569	A2915	A3151	A3744
A0118*	A0978	A2715*	A2923*	A3158	A3764
A0119	A1069	A2717*	A2933	A3194	A3781
A0151	A2353	A2734*	A3009	A3202	A3806
A0168	A2354	A2755*	A3093	A3223	A3809
A0229	A2361	A2764*	A3094*	A3264	A3822
A0295	A2362	A2765	A3108	A3341	A3825
A0303	A2383	A2778*	A3111	A3354	A3827
A0367	A2401	A2799*	A3112	A3528	A3864
A0380*	A2426	A2800*	A3122*	A3559	A3897
A0420	A2436	A2854	A3128	A3703	A3921
A0514	A2480	A2871*	A3141	A3705	

3.1. The cross-correlation between the ENACS and COSMOS catalogues

First, we cross-correlated the galaxies in the ENACS catalogue with the galaxy catalogues for the relevant sections of the COSMOS catalogue (kindly provided by H.T. MacGillivray). Since it was not clear, a priori, to what extent the positional systems in both catalogues are indeed

identical, we first determined the optimum maximum difference in position required for the cross-identification. It appears that a maximum position difference of 7 arcsec must be allowed in order not to miss plausible identifications. However, the surface densities of ENACS and COSMOS galaxies are such that the number of galaxies that is cross-identified does not change significantly if one increases the maximum allowed position difference to ≈ 50 arcsec. In other words: chance coincidences start to be important only for position differences larger than $\sim$50 arcsec.

When preparing the galaxy catalogues for the Optopus observations we limited the selection to the $30-50$ brightest galaxies within the Optopus apertures on survey plates which, for the large majority of the ENACS clusters, are identical to the plates that were scanned for the COSMOS catalogue. Therefore, it is not very meaningful to ask which fraction of all galaxies in the COSMOS catalogue appears in the ENACS. The reason is that this fraction will depend on the effective magnitude limit of our galaxy samples which varies significantly between clusters (the magnitude distributions of the COSMOS and ENACS galaxies, which describe the completeness of the ENACS samples are discussed in Sect. 4.2). Furthermore, the success-rate of the Optopus spectroscopy decreases towards fainter magnitudes (see Fig. 4).

However, it is interesting to ask the complementary question: viz. what fraction of the ENACS galaxies do not appear in the COSMOS catalogue. That some ENACS galaxies (which through the spectroscopy have been "proven" to be galaxies) will not be found in the COSMOS catalogue is to be expected. Heydon-Dumbleton et al. (1989) have estimated that the EDSGC is >95% complete at $b_j = 20.0$, and by determining the fraction of ENACS galaxies not found in the COSMOS catalogue we can provide independent evidence about the completeness of the COSMOS catalogue and its EDSGC subset; or more precisely: at least of those areas that contain rich clusters.

Two of the 77 clusters for which we have COSMOS data, viz. A2502 and A3144, have less than 4 ENACS galaxies, and we have not used those in the following analysis. That leaves 75 clusters which contain, in the areas of overlap between COSMOS and ENACS (which is not always the entire Optopus area) a total of 3896 ENACS galaxies. All these ENACS galaxies are well above the magnitude limit of the COSMOS catalogue. For 357 ENACS galaxies, there is no COSMOS counterpart within 7 arcsec; of these 357 galaxies, 226 do have a nearest neighbour between 7 and 100 arcsec (almost exclusively at more than 50 arcsec), while the remaining 131 have a nearest neighbour at more than 100 arcsec. Taken at face value, these numbers would seem to indicate that the COSMOS catalogue is 91% rather than >95% complete, at the magnitude limit of the ENACS samples which is generally 0.5 to 1.0 mag brighter than $b_j = 20.0$.

This result is somewhat unexpected, but it must be realized that the two completeness estimates refer to slightly different parts of the COSMOS catalogue. Whereas the estimate by Heydon-Dumbleton et al. is the average for the entire EDSGC, our estimate refers to areas with high surface density in the COSMOS catalogue, where it may be more difficult to obtain the same completeness level as in the field. In addition, it is likely that the completeness of the COSMOS catalogue depends somewhat on galactic latitude, local galaxy surface density etc. Therefore, the two completeness estimates need not be really discordant.

We have checked whether the EDSGC is more complete than the total COSMOS catalogue. This appears not to be the case. Of the 357 ENACS galaxies without COSMOS counterpart 92 are in the 15 clusters with EDSGC data, which contain 805 ENACS galaxies in total. Consequently, 265 ENACS galaxies in the other 60 clusters (with a total of 3091 ENACS galaxies) have no COSMOS counterpart. In other words: the completeness estimates for the EDSGC and the rest of the COSMOS catalogue are essentially the same, viz. 89 and 91%.

One might naively expect that the relatively high surface density of, especially, bright and very extended galaxies could be the main reason why some ENACS galaxies do not appear in the COSMOS catalogue. In constructing the ENACS catalogues, plates of all clusters were inspected visually to ensure that the latter were included as much as possible. It is conceivable that the pattern recognition software used in constructing the COSMOS catalogue had some problems in recognizing, especially the brighter, late-type galaxies (we have seen several examples of this, e.g. in A3822). Yet, this effect does not seem to be the main cause for the apparent incompleteness of the COSMOS catalogue. The magnitude distribution of the 357 ENACS galaxies without COSMOS counterparts is virtually the same as that of the other 5258 ENACS galaxies (see Fig. 1), and there is at most a small "excess" of brightest galaxies among the 357 ENACS galaxies without a counterpart in the COSMOS catalogue.

For the 75 clusters used in the comparison, the overall fraction of ENACS galaxies that have no COSMOS counterpart is 9%. For individual clusters the fraction varies between $\sim 4\%$ and $\sim 30\%$. The clusters with smaller number of galaxies show somewhat larger fractions of "missing" COSMOS galaxies, probably mostly as a result of discretization effects due to small numbers.

3.2. Positions

The sample of 3896 galaxies (in 75 clusters) for which the position difference between COSMOS and ENACS is less than 7 arcsec, has been used to investigate the relation between the positional systems in the two sets of data. There could be differences on scales of a few arcsec, because the astrometry for ENACS was done on fairly small sections of the same Schmidt plates for which, in the COSMOS

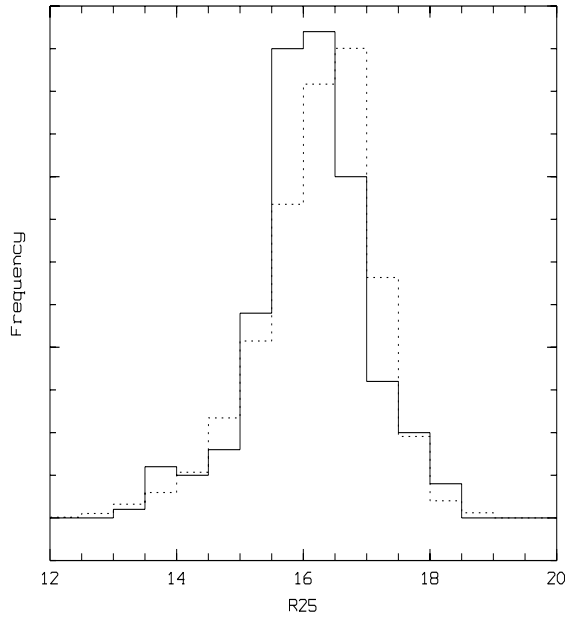

Fig. 1. The normalized distribution wrt apparent magnitude (R_{25}) for the 357 ENACS galaxies without a counterpart in the COSMOS catalogue (solid histogram). For comparison, the normalized R_{25} distribution for the other 5258 ENACS galaxies is shown (dashed histogram)

catalogue, one overall solution was made. However, it appears that such differences are small. The average offsets per cluster are between −2 and +2 arcsec, in both coordinates, and the rms position offset is slightly less than 1 arcsec. In the clusters themselves, the position differences for individual galaxies are of the same order. The overall distribution of position differences, made with all galaxies in common between ENACS and COSMOS (taking out the average, small offset for each cluster), is well described with a Rayleigh distribution with a dispersion of 0.9 arcsec.

For 3 clusters, viz. A3128, A3354 and A3744, all of which were observed with more than one Optopus plate, there is some evidence for an offset of the positions in one Optopus area wrt those in the other Optopus areas. The offsets are probably due to the fact that the astrometry for the different Optopus areas within a cluster was not always based on the same set of standard stars. However, the offsets are small, viz. at most 2.5 arcsec, and often it is not possible to be sure which positions are correct. Although the offsets are probably significant, we have not attempted to correct them; fortunately they are of the same order as the offsets between different clusters, as well as the random position errors.

3.3. Magnitudes

3.3.1. Summary of the ENACS photometry

For the 3896 galaxies that we used in Sect. 3.2, we have also analyzed the relation between the R_{25} magnitudes in the ENACS catalogue and the b_j magnitudes of the COSMOS catalogue. Before we can discuss the results, we must briefly summarize how the ENACS R_{25} magnitudes were derived.

When we produced the galaxy catalogues for the Optopus spectroscopy, by scanning the copies of survey plates with the Astroscan measuring machine, we also obtained accurate photographic photometry. The survey plates that we used, and on which the photographic photometry was done (by measuring the sum of photographic densities, i.e. approximately the amount of silver in the galaxy image), were of two kinds. First, and for most clusters, we used film copies of the SERC survey (with green-sensitive IIIa – J emulsion) and secondly, for the other clusters, we used glass copies of the red POSS–I plates (with red-sensitive 103a–E emulsion).

This photographic photometry was calibrated with CCD-imaging. Because of the limited amount of time available, we did most of our CCD-imaging in R-band and only a small fraction in (the more time-consuming) B-band. Even so, we only managed to calibrate the photometry of about 40 clusters. For those, we determined and applied individual zero-points, while for the other clusters we applied the average calibration curve for the clusters *with* CCD-calibration (see Paper I).

In the case of the IIIa-J plates, we actually measured a photographic b_j magnitude, which we transformed into a calibrated R_{25} magnitude, by effectively subtracting the average apparent $b_j - R_{25}$ colour of *those galaxies that were used for the calibration.* In other words: for the IIIa–J plates, the R_{25} magnitudes are, in effect, b_j magnitudes on a pseudo R_{25}-scale, so that differences in the ENACS R_{25}-values are in reality differences in b_j. On the other hand: for the red POSS–I plates, we really calibrated photographic R-magnitudes with R-magnitudes derived from the CCD-imaging, and differences in ENACS R_{25} are differences in real R_{25}.

In Table 4 we indicate, for each of the 107 clusters in the ENACS, on which type of optical material the magnitudes are based and how these were calibrated. In this table, we indicate if the R_{25}-magnitudes are pseudo R_{25}-values (indicated by G, corresponding to IIIa–J) or real R_{25}-values (indicated by R, corresponding to 103–E), and whether the zero-point that we applied was the average value (a), or individually determined from the CCD-calibration (i).

3.3.2. Comparison of ENACS and COSMOS photometry

As explained above, the comparison between the COSMOS b_j and the ENACS R_{25} magnitudes for

Table 4. The magnitude types and offsets

A0013	G	a	A0087	R	a	A0118	G	a
A0119	R	a	A0151	R	i	A0168	R	i
A0229	R	a	A0295	R	i	A0303	R	a
A0367	G	i	A0380	G	a	A0420	R	a
A0514	G	i	A0524	G	a	A0543	G	a
A0548	G	a	A0754	R	i	A0957	R	i
A0978	R	i	A1069	R	i	A1809	R	i
A2040	R	i	A2048	R	i	A2052	R	a
A2353	R	a	A2354	R	a	A2361	R	a
A2362	R	a	A2383	G	i	A2401	G	a
A2426	R	i	A2436	R	a	A2480	G	i
A2500	G	a	A2502	R	a	A2569	R	a
A2644	R	a	A2715	R	a	A2717	G	i
A2734	G	i	A2755	G	a	A2764	G	i
A2765	G	a	A2778	G	a	A2799	G	a
A2800	G	a	A2819	G	i	A2854	G	a
A2871	G	a	A2911	G	a	A2915	G	i
A2923	G	a	A2933	G	a	A2954	G	a
A3009	G	i	A3093	G	a	A3094	G	i
A3108	G	i	A3111	G	a	A3112	G	i
A3122	G	i	A3128	G	i	A3141	G	i
A3142	G	i	A3144	G	a	A3151	G	a
A3158	G	i	A3194	G	a	A3202	G	a
A3223	G	i	A3264	G	i	A3301	G	a
A3341	G	a	A3354	G	a	A3365	G	a
A3528	G	i	A3558	G	a	A3559	G	a
A3562	G	a	A3651	G	i	A3667	G	i
A3677	G	a	A3682	G	a	A3691	G	i
A3693	G	a	A3695	G	a	A3696	G	a
A3703	G	a	A3705	G	a	A3733	G	a
A3744	G	a	A3764	G	a	A3781	G	a
A3795	G	i	A3799	G	a	A3806	G	a
A3809	G	i	A3822	G	i	A3825	G	a
A3827	G	a	A3864	G	i	A3879	G	a
A3897	G	a	A3921	G	a	A4008	G	a
A4010	G	a	A4053	G	a			

galaxies for which we did the photographic photometry on the *red POSS–I plates*, is a comparison between magnitudes in different spectral bands. Such a comparison therefore involves the individual colours of *all galaxies*, as well as an offset (i.e. the average colour of the *calibrator galaxies*). In Fig. 2 we show the relation between b_j and R_{25} for the galaxies for which $b_j - R_{25}$ measures a real colour. In this figure we have corrected the b_j magnitudes by 1.5 mag, which approximately takes into account the average colour of the galaxies. The result is quite reassuring: there do not appear to be serious problems with either of the magnitude scales, and the fairly wide colour distribution of the galaxies is clearly visible.

On the other hand, the comparison between b_j and R_{25} magnitudes for galaxies measured on *IIIa–J plates*, is a comparison between two measures of the same thing, because R_{25} is actually b_j on a pseudo R_{25} scale. In this

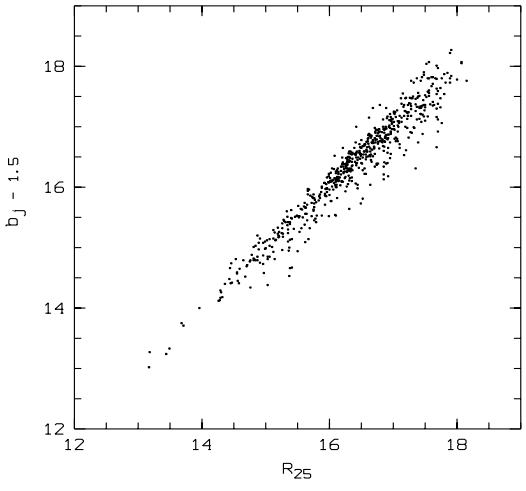

Fig. 2. The relation between $b_j - 1.5$ (i.e. the COSMOS b_j magnitude corrected for the approximate average colour) and R_{25}, for the galaxies in the clusters for which R_{25} was based on 103a–E plates

case, the offset between b_j and R_{25} is equal to the *average colour of the galaxies that were used for calibration*. In addition, there is some noise due to different sampling of the brightness distributions, small differences in the definition of the aperture over which the brightness was integrated, and possibly some noise generated by the two measuring machines.

The difference between the two cases (b_j vs. real R_{25} and b_j vs. pseudo R_{25}) is clearly visible in Fig. 3, where we show two distributions of relative colour, viz. $b_j - R_{25}$ of an individual galaxy referred to the average colour $< (b_j - R_{25}) >_{\rm cluster}$ of its cluster. The upper histogram refers to 59 "clusters" scanned on IIIa–J plates (one cluster, A3264, was not included in the upper histogram because it has only 5 galaxies in common between ENACS and COSMOS, so the average colour is not very well defined); the lower histogram refers to the 17 clusters with photographic photometry on 103a–E plates.

It is clear that the lower histogram is significantly wider than the upper one, as a result of the appreciable range of galaxy colours. This is indicated not only by the dispersions in $b_j - R_{25} - < b_j - R_{25} >_{\rm cluster}$, which are 0.23 and 0.11, respectively but also by the long tails in the lower distribution. The dispersion for the IIIa–J plates, of 0.11 mag, is quite satisfactory in view of the estimated random errors in the individual magnitude estimates of about 0.15 mag.

We have checked if there are differences between the two subsets of the COSMOS catalogue, i.e. EDSGC and

non-EDSGC and, as expected, we indeed find that the EDSGC subset has a better magnitude-calibration than the non-EDSGC subset. This is apparent from the following numbers: if one makes separate versions of the upper histogram in Fig. 3, for EDSGC and non-EDSGC we find dispersions of 0.097 and 0.114 respectively. Even stronger evidence is provided by the dispersions in the individual values of $< (b_j - R_{25}) >_{\rm cluster}$ which are 0.25 and 0.37 for EDSGC (14 clusters) and non-EDSGC (44 clusters) respectively. However, within the errors the average colours are the same, viz. 1.54 ± 0.06 for the EDSGC and 1.44 ± 0.06 for the non-EDSGC part of the COSMOS catalogue.

Note that in the previous paragraph we have tacitly assumed the ENACS magnitudes to provide a reference system for the COSMOS magnitudes. However, the distribution of the average colours $< b_j - R_{25} >_{\rm cluster}$, in principle also contains information on the quality of the ENACS magnitude calibration. As with the magnitudes, the meaning of these average colours depends on the type of photometric photometry that was calibrated with the R-band CCD-imaging

For clusters with Astroscan data from 103a–E plates, $< b_j - R_{25} >_{\rm cluster}$ is a *real* colour, viz. the average colour of *all* galaxies in the cluster for which we have R_{25} as well as a b_j available (i.e. not just those used in the calibration). Differences in average colour between clusters can thus be due to significantly different total galaxy populations in different clusters. In addition, the zero-point of the calibration for a given cluster is not known with infinite precision; however, zero-point errors are measurement- and limited statistics- errors only, and are not dependent on the colours of the calibrating galaxies.

There are 17 clusters for which we used 103–E plates for the photographic photometry; 6 of these were calibrated individually with CCD-imaging, while for the other 11 clusters we applied the average relation derived for those 6. For the 6 clusters we find average cluster colours and dispersions of 1.69 and 0.24, with the offsets applied. If we do not apply the individual offsets, we find 1.78 and 0.27. Clearly, the statistics is not overwhelming, and the assumption of a universal $(b_j - R_{25})$-distribution may not be a very good one for such a limited number of clusters. Yet, there is some evidence that the application of the individual zero-points for the 6 clusters makes sense as the dispersion around the average value of $< b_j - R_{25} >_{\rm cluster}$ increases from 0.24 to 0.27 (and from 0.22 to 0.32 for the 4 clusters with at least 5 galaxies with CCD-imaging), if one does not apply the 6 individual zero-points. However, we note that the dispersion of the mean colours of the 11 clusters for which we applied the average calibration, is only 0.21. This must mean that differences in the average real colours of the calibrator galaxies in the individually calibrated clusters do indeed play a rôle. On the other hand, the latter also indicates that the average calibration is quite good.

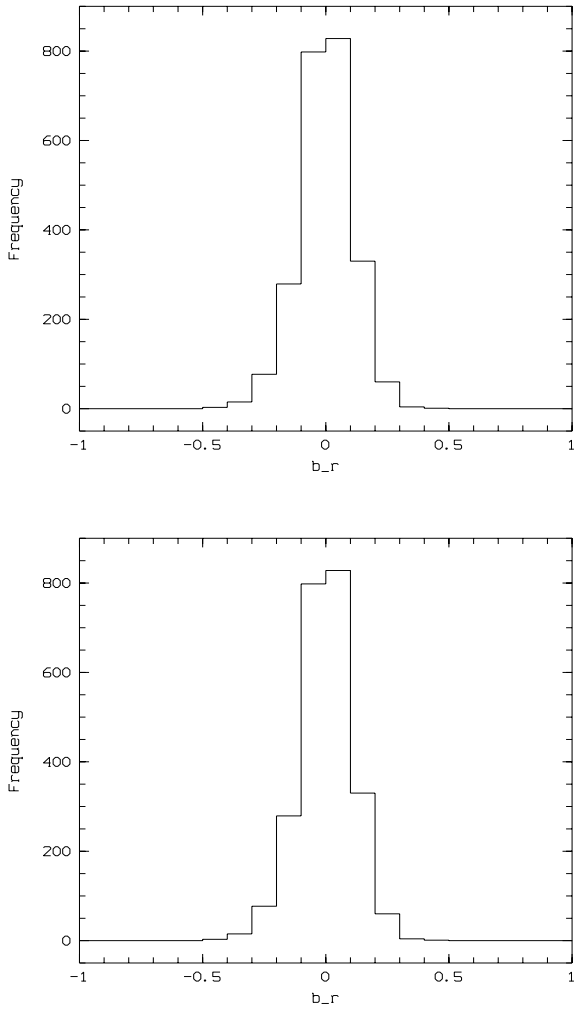

Fig. 3. The distribution of the colour difference $(b_j - R_{25})$ for galaxies that are common to COSMOS (the source of b_j) and the ENACS (the source of R_{25}). Note that all colours are referred to the average colour $< (b_j - R_{25}) >_{\rm cluster}$ of the "cluster" to which the galaxy belongs. The upper histogram is for "clusters" for which R_{25} was estimated from IIIa–J plates, the lower histogram for clusters for which R_{25} was measured on 103a–E plates

On the other hand, for clusters with Astroscan data from IIIa–J plates, we are *not* dealing with *real* average galaxy colours because the measured b_j and the pseudo R_{25} magnitudes are based on the *same* images on the *same* IIIa–J plates. Therefore the average colour $< b_j - R_{25} >_{\rm cluster}$ in this case does not reflect the average colour of the total galaxy population, but only the real average colour *of the calibrating galaxies*. Especially when the calibration is based on a fairly small number of galaxies, differences in the real average colour of the

calibrating galaxies may be as important as errors in the determination of the zero-point.

In the COSMOS-ENACS comparison 58 clusters have photographic photometry from IIIa–J plates; for 23 of those an individual CCD-calibration was available. From the average colours of the latter, it is immediately clear that there is a serious problem with the calibration for A3559 (and therefore also A3558 and A3562, which have identical calibration). The apparent value of $< b_j - R_{25} >_{\rm cluster}$ for A3559 is 0.1 rather than about 1.5, as found for the other clusters. This means that the large zero-point correction of 1.7 that we found must indeed have been incorrect (as we already suspected in Paper I, but could not "prove" without the COSMOS magnitudes). Therefore, in the ENACS catalogue we have, for A3558, A3559 and A3562, not applied the zero-point derived in Paper I, but the average zero-point.

The remaining 22 clusters with individual calibration show a clear relation between the apparent value of $< b_j - R_{25} >_{\rm cluster}$ and the number of galaxies with CCD-imaging, on which the calibration is based. The observed average values are 1.62 for clusters with $N > 6$ and 1.24 for clusters with $N \leq 6$. When the number of calibrating galaxies is low one is more likely to have a difference in average colour between the calibrating galaxies and the (much more) numerous galaxies used in the COSMOS-ENACS comparison. That this should produce a colour bias is not immediately evident, but not difficult to explain either. When the distribution of galaxy colours is skewed (see Fig. 2), or if a magnitude limit in one of the colours induces a colour selection, a bias could easily result. For the 11 clusters with $N \leq 6$, the average value of $< b_j - R_{25} >_{\rm cluster}$ differs so systematically and considerably from the average value for the other clusters that we have decided, in those cases, not to apply the individual zero-points derived in Paper I. The clusters in question are: A2480, A2717, A2734, A2915, A3009, A3094, A3108, A3141, A3809, A3822 and A3864.

For the 11 individually calibrated clusters with $N > 6$, the dispersion in average colour is 0.17, which must be compared with the corresponding value of 0.25 for the 36 clusters without individual calibration. So, indeed there is some evidence that the individual zero-points are worth applying, even though they differ only by a few tenths from the average zero-point. However, if one applies the average zero-point for the 11 calibrated clusters, the dispersion in the average colour does not increase noticeably. This is consistent with the fact that the dispersion is dominated by the 36 clusters without individual calibration.

In summary, we conclude from the comparison of the COSMOS and ENACS magnitudes that:
– the average calibration applied to the majority of the ENACS clusters is well supported by the magnitudes in the COSMOS catalogue
– the zero-points obtained for individual clusters are somewhat, but not very much, better than the average zero-point derived from all clusters with photometric calibration
– we found good reasons for not applying the individual zero-points derived in Paper I of 14 clusters: A3558, A3559, A3562 and the 11 clusters listed above.

4. Selection and completeness

4.1. Selection in position

The ENACS galaxy samples were designed to constitute magnitude-limited subsets of the general galaxy population in the areas defined by the Optopus plates (see Table 5 for the centres of these circular, 31′-diameter, areas). In Sect. 3.1 we found that the ENACS samples contain a few galaxies (for which we measured an ENACS redshift, and therefore presumed real) which are not in the COSMOS catalogue. Apart from this fairly minor effect, the ENACS galaxy samples are indeed subsets of the COSMOS catalogue. A question which may be important for some types of analysis, is whether the ENACS galaxy samples, which were selected on magnitude, form *unbiased* subsets of the COSMOS catalogue *as far as position is concerned*. In other words: does the surface density of the ENACS galaxies more or less follow that of the COSMOS galaxies within the areas covered by the Optopus plates.

To investigate this question we have applied a 2-D Kolmogorov-Smirnov test (Fasano & Franceschini 1987) to the ENACS and COSMOS galaxy distributions in the solid angle of the ENACS survey (either a single Optopus area, or the union of several Optopus areas). In order to make the test meaningful we have applied it to subsamples of both the ENACS and COSMOS catalogues complete to magnitude limits, $R_{25,\rm lim}$ and $b_{j,\rm lim}$ that differ by the average value of $< b_j - R_{25} >$ for which we took 1.5. For each cluster, we applied the test for five pairs of $(R_{25,\rm lim}, b_{j,\rm lim})$, with $R_{25,\rm lim} = 16.5(0.5)18.5$. Clearly, if $R_{25,\rm lim}$ becomes fainter than the actual magnitude limit of the ENACS data in a given cluster (see Sect. 4.2), the ENACS galaxies represent a progressively smaller fraction of the COSMOS sample, and there will be a natural tendency for the two projected distributions to become different, if they were not so already at brighter limits.

We have analyzed for each cluster the KS-probabilities at the five different magnitude limits, and we conclude that for almost all clusters, the galaxy distributions in the ENACS and COSMOS catalogues are not different at a confidence level of more than 95%. There are only three clusters, viz. A3705, A3809 and A3825, for which it appears that the ENACS galaxy distribution differs from that of the COSMOS galaxies at more than 95% confidence level. In all three cases, inspection of contour maps of galaxy surface density visually supports this conclusion: the ENACS galaxies are relatively abundant at the edges of the concentrations present in the COSMOS surface density. In addition, there is one cluster, A3822, for

which there is marginal evidence for a biased selection. However, in that case there is a secondary concentration in the COSMOS data which is not present in the distribution of the ENACS galaxies. For contour maps of projected galaxy density based on the COSMOS catalogue, we refer the reader to Adami et al. (1998).

4.2. Selection in magnitude for clusters with COSMOS data

In Fig. 1 we have given the overall magnitude distribution of the galaxies for which the ENACS has yielded a redshift. This distribution shows that on average the redshift catalogues start to become incomplete below $R_{25} \sim 17$, but that the fraction of ENACS galaxies with R_{25} between 17 and 19 is non-negligible. The decrease in the number of galaxies beyond $R_{25} \sim 17$ is the result of two factors. First, the galaxy catalogues that we prepared have (fairly sharp) magnitude cut-offs at R_{25} between about 17.5 and 19.0. Second, our success in obtaining redshifts decreases quite strongly for $R_{25} \gtrsim 17$.

In Fig. 4 we show as a function of R_{25}, for the ENACS as a whole, the ratio of the number of galaxies for which the ENACS observations have yielded a redshift and the total number of galaxies that we observed in the ENACS. In other words: Fig. 4 shows our success-rate of obtaining a redshift as a function of magnitude. Figure 4 therefore quantifies our discussion in Sect. 5.5 of Paper I, where we already mentioned that our maximum success-rate was about 80%. The strong decrease for $R_{25} \gtrsim 17$ is due to the smaller S/N-ratio of the absorption lines in the spectra of the fainter galaxies. The fact that we do not score 100% for the brightest galaxies must be due to the less-than-ideal match between the diameter of the Optopus fibres and the surface brightness distribution of some of the brightest galaxies, which can have a relatively low central surface brightness.

For some types of discussion it may be necessary to know, as a function of magnitude, the fraction of COSMOS galaxies (i.e. cluster *and* field galaxies) for which we obtained an ENACS redshift. This fraction is shown graphically in Fig. 5, as a function of R_{25}, for all 73 clusters for which this fraction could be meaningfully determined. For 4 clusters no distributions are given because either the number of ENACS galaxies is very small (A2502 and A3144), or the overlap between ENACS and COSMOS data is too limited (A0543 and A2915). Rather than show the fraction itself, we give the magnitude distributions of ENACS and COSMOS galaxies, both normalized to the number of ENACS galaxies in the most populated 0.5-mag bin. The two magnitude distributions refer to the same solid angle, i.e. the overlap "area" between the two surveys.

In general, the ENACS magnitude distribution coincides with, or falls below, that based on COSMOS, as expected. However, in some cases, the ENACS distribution

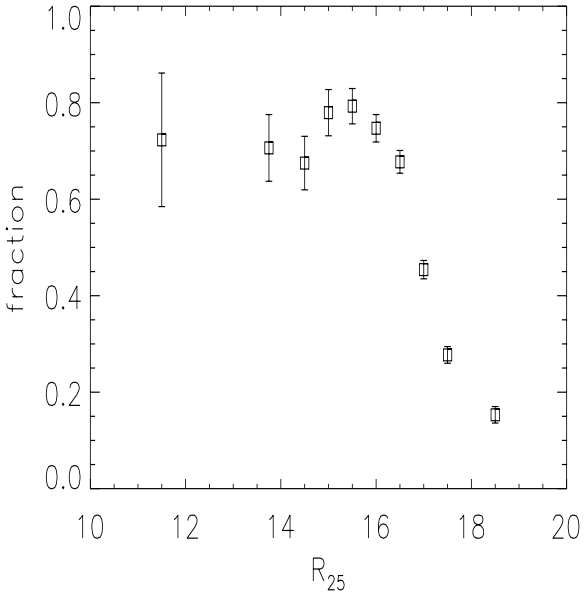

Fig. 4. The ratio of the number of galaxies for which the Optopus observations have yielded a redshift and the total number of galaxies observed in the ENACS, as a function of R_{25}

exceeds that based on COSMOS, particularly at brighter magnitudes. One factor that may contribute to this is that some of the bright ENACS galaxies are not in the COSMOS catalogue (see Sect. 3.1). Another reason for this small inconsistency which appears only occasionally, is that the two distributions are on different magnitude scales. The COSMOS distributions have been brought to the R_{25} scale by applying a correction for the average $b_j - R_{25}$ colour for the *entire* ENACS survey.

Figure 5 shows that, with one or two exceptions, the ENACS galaxy samples are essentially complete, magnitude-limited, subsets of the COSMOS samples up to an R_{25} of 16.5 ± 0.5 (within the ENACS apertures!). The fainter galaxies can, of course, be used in discussions for which the completeness of the galaxy sample is not important.

4.3. Magnitude and redshift selection for the ENACS as a whole

For several types of analysis it may be useful to have analytic expressions for the cut-offs towards faint magnitudes and higher redshifts for the ENACS as a whole. For the analysis of these cut-off functions we have restricted ourselves to the galaxies that are not in the main system, i.e. those in the field and in secondary systems. This avoids possible complications due to the rather uneven redshift

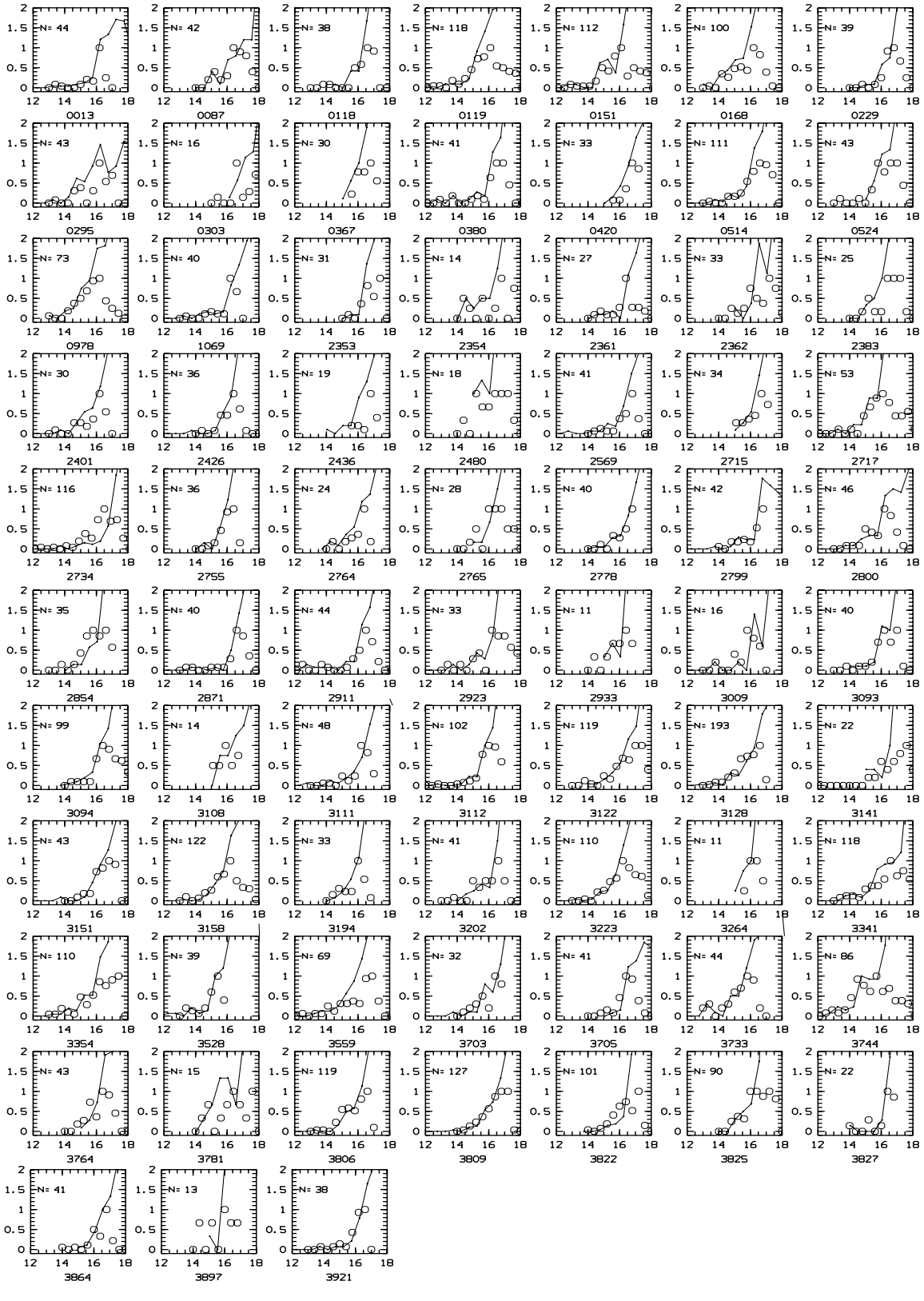

Fig. 5. The normalized magnitude distributions of COSMOS (line) and ENACS (circles) galaxies in the overlap areas between the COSMOS and ENACS catalogues, for 73 clusters (ACO number is given below frame; number of ENACS galaxies – N – shown in frame). Magnitudes are on the R_{25} scale (COSMOS b_j magnitudes have been corrected for the average $b_j - R_{25}$ colour). Normalization is wrt the most populated 0.5-mag bin in the distribution for the ENACS galaxies

distribution of galaxies in the rich systems. For reasons that are not important here, the analysis was done on a representative subset of 65 ENACS clusters, with a total of 681 "field" galaxies. The distribution of those 681 galaxies with respect to apparent (R_{25}) magnitude and redshift is shown in the upper lefthand panel of Fig. 6.

We assume the following model when trying to reproduce this observed distribution:

$$N_{\rm obs}(R_{25}, cz) = N_{\rm int}(R_{25}, cz) \times S_1(R_{25}) \times S_2(cz)$$

in which $N_{\rm int}(R_{25}, cz)$ is the unbiased distribution for a constant luminosity function. In other words: we assume that there are two independent cut-off functions, $S_1(m)$ which describes the magnitude cut-off in the galaxy sample for which we attempted spectroscopy and $S_2(v)$ which describes the succes-rate of obtaining a redshift as a function of velocity.

In the upper righthand panel of Fig. 6 we show a predicted $N_{\rm obs}(R_{25}, cz)$ distribution, calculated *without magnitude or redshift cut-off*, for a sample of 681 galaxies using a Schechter luminosity function with $M_R^* = -22.5$ and $\alpha = -1.25$, and using $m = M + 15 + 5\log(cz) - 5\log h$, to transform from absolute to apparent magnitude. Clearly, this prediction is very different from the observed distribution.

The introduction of a magnitude cut-off of the form

$$\begin{aligned} S_1(R_{25}) \;&=\; 1 && \text{for} \;\; R_{25} \le 16.5 \\ &\quad\; 10^{-1.2(R_{25}-16.5)} && \text{for} \;\; R_{25} > 16.5 \end{aligned}$$

produces the distribution in the lower lefthand panel, which has more or less the correct total magnitude distribution. However, the total redshift distribution extends too much beyond $\approx$ 40 000 km/s.

Finally, the application of a redshift cut-off of the form

$$\begin{aligned} S_2(cz) \;&=\; 1 && \text{for} \;\; cz \le 30\,000 \;\; \text{km/s} \\ &\quad\; \left(\frac{30\,000}{cz}\right)^4 && \text{for} \;\; cz > 30\,000 \;\; \text{km/s} \end{aligned}$$

yields the distribution shown in the lower righthand panel. Note that we do not pretend that this is the best description one may give. However, we have chosen the functional forms of, and the parameters in the cut-off functions not just by looking at Fig. 6. Instead, we have tried to reproduce as closely as possible the observed redshift distributions in several rather narrow magnitude intervals. Short of introducing a possible dependence of e.g. $S_2(v)$ on m etc., we think the selection functions given here provide a sufficiently accurate description of the overall selection functions in the *ENACS as a whole* (but these may not be necessarily correct for individual clusters!).

That the selection functions given here, on the basis of the galaxies in the "field" are at least reasonable is also supported by the following evidence. For the galaxies in the clusters with $v < 30\,000$ km/s, only $S_1(m)$ is relevant.

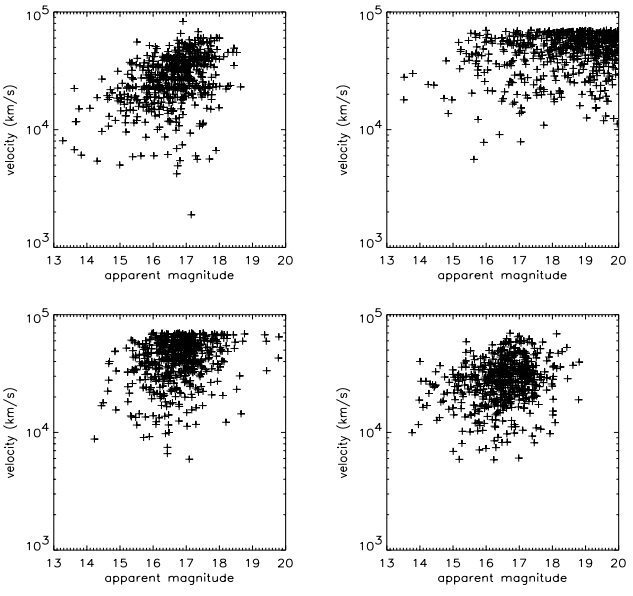

Fig. 6. The distribution of the galaxies that are not in the main system (i.e. in the "field") wrt to magnitude, R_{25}, and redshift. The upper lefthand panel shows the observed distribution for 681 galaxies in 65 clusters. The upper righthand panel gives the result of a simulation for the same number of galaxies, without cut-offs in magnitude or redshift. The lower lefthand panel also results from a simulation, with the magnitude cut-off described in the text, but without redshift cut-off. The lower righthand panel shows the result of a simulation with the magnitude and redshift cut-off functions described in the text

Using again a Schechter luminosity function, with $M_R^* = -22.5$ and $\alpha = -1.25$, we predict that the average number of observable galaxies in a cluster depends on the redshift of the cluster as z^{-1}. This is consistent with what we find for the main systems in ENACS (see e.g. Paper I).

5. Some important properties of the ENACS catalogue

By themselves, the 107 clusters for which data is given in the present catalogue do not form a complete, volume-limited sample of $R_{\rm ACO} > 1$ Abell clusters. However, the ENACS was designed to establish, *in combination with data available in the literature*, a database for a complete, "local" sample of $R_{\rm ACO} > 1$ Abell clusters with redshifts < 0.1. In Sect. 2.2 of Paper II, the resulting complete sample of 128 $R_{\rm ACO} > 1$ clusters (with $z \le 0.1$, and in the solid angle defined by $b \le -30°$ and $-70° \le \delta \le 0°$) has been described.

For 78 of these clusters, data were provided exclusively by the ENACS, while for 5 additional clusters the ENACS contributed to existing data. As discussed in Paper II, these 128 clusters represent a total of 158 $\pm$ 10 clusters in a volume of 9.2 10^6 h^{-3}Mpc^3. One of the results of

the ENACS observations is that for 83 of the 128 clusters we have an improved estimate, through the redshifts, of the contribution to the cluster richness from background galaxies.

In the ENACS cluster sample there is a general bias against clusters with $z \leq 0.04$, as those are too extended for efficient observation with the Optopus spectrograph. On the other hand, outside the "cone" described above, we could not (and did not) seek to reach completeness, and as a result clusters with $z \sim 0.05$ are overrepresented in the ENACS, and for $z \gtrsim 0.06$ the ENACS is only complete within the "cone".

When selecting galaxy subsets from the ENACS catalogue it must always be remembered that, at the fainter magnitudes, galaxies without emission lines are significantly discriminated against in comparison with galaxies that have clear emission lines (see Sect. 2.5 of Paper III). As a result of the differences in the projected distributions of galaxies with and without emission lines, the application of a limit to the projected distance from the cluster centre influences the mix between early- and late-type galaxies (Sect. 5, ibid.).

6. Summary and conclusions

We have presented and described the ENACS redshift catalogue, as well as several aspects of the survey that are relevant in statistical use of the catalogue. From a comparison with the COSMOS Galaxy Catalogue, we conclude that the positional system of the ENACS agrees very well with that of the COSMOS catalogue. A comparison between the magnitude systems of ENACS and COSMOS catalogues shows satisfactory agreement, although the comparison has made us revise the zero-points of the magnitude scales of 14 clusters. Finally, we discuss the way in which the samples of ENACS galaxies are subsets of the total galaxy samples from the COSMOS catalogue. It appears, that the ENACS samples are fair approximations to magnitude limited subsets of the COSMOS catalogue, although our success in obtaining redshifts decreases markedly towards the fainter magnitudes.

Acknowledgements. We gratefully acknowledge the substantial support given to this project by ESO, without which the construction of a dataset for a large, volume-limited cluster sample would have been impossible. We thank Pascal de Theije for providing the analytic description of the completeness in Sect. 4.3. We thank Harvey MacGillivray for providing access to sections of the COSMOS and EDSGC Galaxy Catalogues. We thank the referee, L. Guzzo, for useful comments about the COSMOS catalogue.

We thank our collaborators on what used to be called the ESO Cluster Key Programme, for their contributions.

PK, RdH and AB acknowledge financial support from the Leids Kerkhoven-Bosscha Fonds. AM, AB, CA and PK acknowledge financial contributions from the French GDR Cosmologie and from INSU. JP acknowledges support from the Spanish DCICYT (program PB93-0159).

References

Abell G.O., 1958, ApJS 3, 211
Abell G.O., Corwin H.G., Olowin R.P., 1989, ApJS 70, 1
Adami C., Mazure A., Biviano A., Katgert P., Rhee G., 1997, A&A (in press)
Adami C., Mazure A., Katgert P., Biviano A., 1998, A&A (submitted)
Avila G., D'Odorico S., Tarenghi M., Guzzo L., 1989, ESO Messenger No. 55, p. 62
Beers T.C., Forman W., Huchra J.P., Jones C., Gebhardt K., 1991, AJ 102, 1581
Biviano A., Katgert P., Mazure A., et al., 1997, A&A 321, 84 (Paper III)
Borgani S., Moscardini L., Plionis M., et al., 1997, New Astr. 1, 321
den Hartog R., 1997, MNRAS 284, 286
den Hartog R., Katgert P., 1996, MNRAS 279, 349
de Theije P.A.M., Katgert P., 1998, A&A (submitted)
Dressler A., 1980, ApJS 42, 565
Dressler A., Shectman S.A., 1988, AJ 95, 284
Faber S.M., Dressler A., 1977, AJ 82, 187
Fadda D., Girardi M., Giuricin G., Mardirossian F., Mezzetti M., 1996, ApJ 473, 670
Fasano G., Franceschini A., 1987, MNRAS 225, 155
Girardi M., Escalera E., Fadda D., et al., 1997, ApJ 482, 41
Godwin J.G., Peach, J.V., 1977, MNRAS 181, 323
Heydon-Dumbleton N.H., Collins C.A., MacGillivray H.T., 1989, MNRAS 238, 379
Hill J.M. Oegerle W.R., 1993, AJ 106, 831
Huchra J.P., Geller M.J., Corwin H.G., 1995, ApJS 99, 391
Katgert P., Mazure A., Perea J., et al., 1996, A&A 310, 8 (Paper I)
Kent S.M., Gunn J.E., 1982, AJ 87, 945
Lund G., 1986, ESO Operating Manual No. 6
Maddox S.J., Efstathiou G., Sutherland W.J., Loveday J., 1990, MNRAS 243, 692
Malumuth E.M., Kriss G.A., Van Dicke Dixon W., Ferguson H.C., Ritchie C., 1992, AJ 104, 495
Mazure A., Katgert P., den Hartog R., et al., 1996, A&A 310, 31 (Paper II)
Quintana H., Melnick J., Infante L., Thomas B., 1985, AJ 90, 410
Tonry J., Davis M., 1979, AJ 84, 1511
Wallin J.F., Yentis D., MacGillivray H.T., Bauer S.B., Wong C.S., 1994, BAAS 184, No. 27.04
Zabludoff A.I., Geller M.J., Huchra J.P., Vogeley M.S., 1993, AJ 106, 1273